

## INTERNATIONAL ULTRAVIOLET EXPLORER OBSERVATIONS OF HYADES STARS

MARIE-CHRISTINE S. ZOLCINSKI,<sup>1</sup> SPIRO K. ANTIOCHOS,<sup>1</sup> ROBERT A. STERN,<sup>2</sup> AND  
 ARTHUR B. C. WALKER<sup>1</sup>

Received 1981 September 21; accepted 1982 January 20

### ABSTRACT

We have obtained short-wavelength, low-dispersion ultraviolet spectra of seven of the brightest X-ray emitting stars in the Hyades cluster with the *IUE* observatory. Four of the stars show evidence of emission lines characteristic of transition region temperatures ( $\sim 30,000$ – $200,000$  K); for the remaining three stars, we derive upper limits for emission-line fluxes. In addition, we have observed three of the above stars with the long-wavelength spectrograph on *IUE* at high dispersion and find evidence for chromospheric emission from the Mg II *h* and *k* lines for two of these objects. Combining the *IUE* results with X-ray observations from the survey of the Hyades with the *Einstein* Observatory carried out by Stern *et al.*, we estimate the differential emission measure function for each of the above stars. We derive constraints on stellar atmospheric parameters (chromospheric pressure, coronal temperature, and “filling factor”) and discuss the implications of our results for models of stellar chromospheres and coronae.

*Subject headings:* clusters: open — stars: chromospheres — ultraviolet: spectra —  
 X-rays: sources

### I. INTRODUCTION

Ultraviolet and X-ray observations of the outer atmospheres of cool stars made with the *IUE* and *Einstein* satellites have recently led to a major reassessment of theoretical models for stellar chromospheres, transition regions and coronae. Previous X-ray stellar surveys (e.g., Vaiana *et al.* 1981; Walter and Bowyer 1981; Stern *et al.* 1981) have indicated that many solar type stars have X-ray luminosities as high as  $10^3$  times that of the Sun. Ultraviolet observations demonstrate that emission-line fluxes from many of these same stars are an order of magnitude or more greater than solar (Linsky 1981; Dupree 1981) and that the transition region line fluxes correlate very well with X-ray fluxes (Ayres, Marstad, and Linsky 1981).

Stern *et al.* (1981) have reported on an extensive soft X-ray survey of the central region of the Hyades cluster with *Einstein*. Their results demonstrate that G dwarfs in the Hyades have typical X-ray luminosities ( $L_x$ )  $\sim 30$  times or more than solar. However, the X-ray spectra can only be roughly determined at this time from the *Einstein* Imaging Proportional Counter data. Thus, in the context of loop models for the corona and transition region, the coronal temperature, area coverage factor, and pressure at the base of the transition region cannot be determined independently. However, far-ultraviolet observations of transition region lines, in conjunction with the X-ray measurements, can be used to constrain these parameters.

In this paper, we discuss *IUE* observations of transition region and chromospheric emission from a group of Hyades dwarfs that are strong X-ray emitters as seen in the Stern *et al.* (1981) survey. In § II, we

describe the observations and compare our results with those from previous *IUE* observations of cool stars. In § III, we discuss the application of static loop models to our data, and in § IV, we present a brief summary of our work.

### II. OBSERVATIONS

The seven selected stars were observed with the short-wavelength prime (SWP) camera on *IUE* at low dispersion ( $\sim 6$  Å resolution from 1175 to 2000 Å). Three of the seven were also observed with the long-wavelength redundant (LWR) camera at high dispersion ( $\sim 0.2$  Å resolution at the Mg II *h* and *k* lines near 2800 Å). The design and operation of the *IUE* satellite is described in Boggess *et al.* (1978*a, b*).

The characteristics of the observed stars are listed in Table 1; the observations are summarized in Table 2; and the spectra are illustrated in Figure 1 for the short-wavelength range and Figure 2 for the long-wavelength Mg II *h* and *k* lines. All the targets were observed through the *IUE* aperture ( $10'' \times 20''$ ). The extracted spectra were corrected to the revised intensity transfer function according to the algorithm proposed by Holm (1979) and then converted to absolute flux units using the Bohlin *et al.* (1980) sensitivity curve.

Proposed line identifications are based on the solar line lists of Burton and Ridgeley (1970) and Doschek *et al.* (1976). The reality of the line features was assessed in a similar manner to that described in Linsky *et al.* (1979). Emission-line fluxes and  $2\sigma$  upper limits include uncertainties due to stellar continuum and instrumental background. In Table 3 we give the measured line fluxes and upper limits to line fluxes at Earth for both the SWP and LWR spectra. We estimate the accuracy of these fluxes to be better than a factor of 2. Also included

<sup>1</sup> Institute for Plasma Research, Stanford University.

<sup>2</sup> Jet Propulsion Laboratory, California Institute of Technology.

TABLE 1  
STELLAR PARAMETERS

Parameter	71 Tau	BD +15°640	70 Tau	BD +14°693	BD +16°592	BD +15°598	BD +16°601
Sp.....	F0 V	F5 V	F7 V	G1 V	G1 V	G5 V	G6 V
$V$ .....	4.50	6.51	6.46	7.62	7.80	8.06	8.12
$B-V$ .....	0.25	0.42	0.49	0.60	0.60	0.63	0.66
$V-R$ .....	0.27	0.40	0.45	0.52	0.52	0.54	0.56
$\phi$ .....	0.66	0.34	0.38	0.26	0.24	0.22	0.22
$v \sin(i)$ (km s <sup>-1</sup> ).....	192	53	15	...	6	...	...
$T_{\text{eff}}$ (K).....	7450	6440	6180	5870	5870	5770	5660
$\log(g)$ (cm s <sup>-2</sup> ).....	4.25	4.3	4.3	4.4	4.4	4.44	4.5

in Table 3 are the soft X-ray fluxes from the selected stars (Stern *et al.* 1981; Zolcinski 1981). Surface fluxes for the four stars in which we detected emission lines, as well as for the quiet Sun, are given in Table 4 using the method described by Ayres, Marstad, and Linsky (1981), which converts fluxes at earth to stellar surface fluxes by estimating the stellar angular diameter from the color index relation of Barnes and Evans (1976).

a) Short-Wavelength Spectra (1175–2000 Å)

Of the three F stars in our observing program 17 Tau (F0 V), BD +15°640 (F5 V), and 70 Tau (F7 V), all but the earliest, 71 Tau, show evidence for far-ultraviolet line emission. N v  $\lambda$ 1240, indicative of gas at a temperature  $T \sim 2 \times 10^5$  K, is present only in the spectrum of 70 Tau, although its measured intensity may be suspect because of nearby geocoronal Ly $\alpha$ . C iv  $\lambda$ 1549 ( $T \sim 1 \times 10^5$  K) is present in both BD +15°640 and 70 Tau at about the same level. C ii  $\lambda$ 1335 ( $T \sim 3 \times 10^4$  K) is also easily identifiable in both spectra. Cooler material ( $T < 10^4$  K) is indicated by the presence of C i  $\lambda$ 1561, 1657 in BD +15°640, but it is not seen in the 70 Tau spectrum. This is somewhat curious in light of the

TABLE 2  
SUMMARY OF IUE OBSERVATIONS

Star	Image	Day (year 1980)	Begin Time (UT)	Exposure (min.)
71 Tau .....	SWP 9855	234	14:47 <sup>a</sup>	3
	...	...	14:57	3
	SWP	236	09:48	20
	LWR 8591	236	09:38	6
BD +15°640 .....	LWR 8572	234	14:19	20
	SWP 9856	234	16:10	96
	SWP 9875	236	10:56	120
	LWR 8573	234	15:35	30
70 Tau .....	SWP 9877	236	17:09	38
	SWP 9853	234	02:36	240
	LWR 9871	234	06:44	30
	LWR 8592	236	16:35	28
BD +14°693 .....	SWP 9876	236	13:28	180
BD +16°592 .....	SWP 9854	234	07:23	400
BD +16°598 .....	SWP 9614	209	16:44	186
BD +16°601 .....	SWP 9612	209	12:46	60
	SWP 9613	209	14:15	120
	SWP 9873	236	02:37	390

<sup>a</sup> Small aperture.

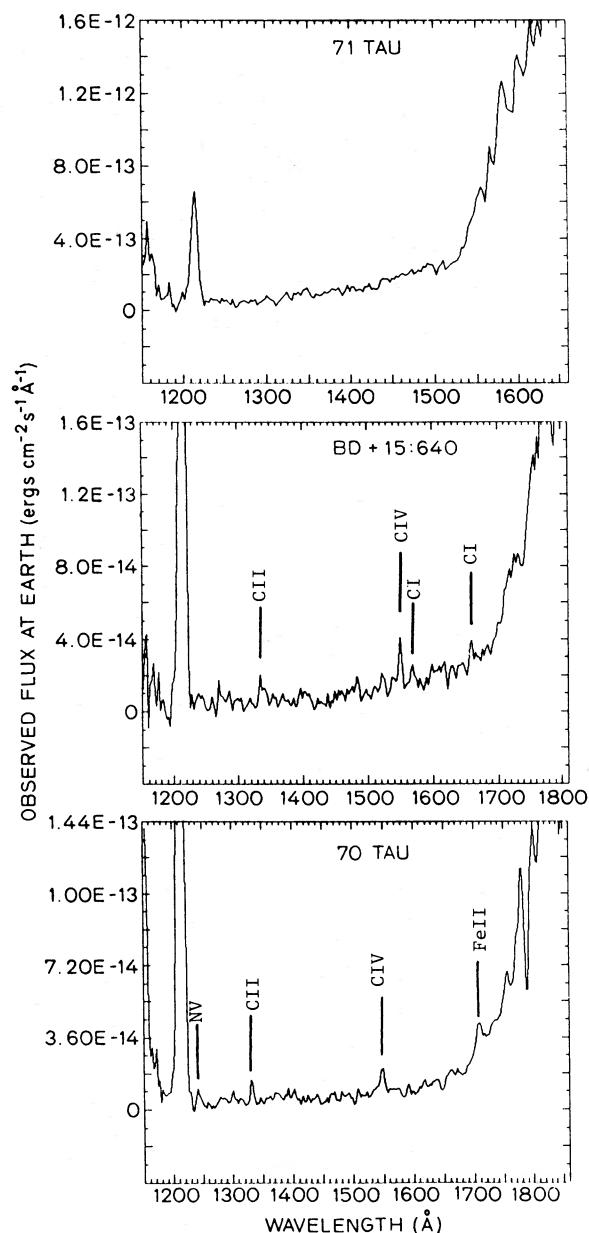


FIG. 1.—IUE short wavelength spectra of the Hyades stars

TABLE 3  
SUMMARY OF OBSERVED EMISSION-LINE FLUXES AT EARTH ( $\text{ergs cm}^{-2} \text{s}^{-1}$ )

$\lambda(\text{\AA})$	Ion	71 Tau	BD +15°640	70 Tau	BD +14°693	BD +16°592	BD +16°598	BD +16°601
1240 .....	N v (1)	<1(-12)	<4(-14)	2.8(-14)	<3(-14)	<3(-14)	<5.5(-14)	<3(-14)
1305 .....	O I (2)	<1(-12)	<4(-14)	2.7(-14)	<3(-14)	<3(-14)	<4.4(-14)	<3(-14)
1335 .....	C II (1)	<1(-12)	7(-14)	5.3(-14)	5.8(-14)	<3(-14)	<5.5(-14)	<3(-14)
1394 .....	Si IV (1)	<1(-12)	<4(-14)	4(-14)	5.0(-14)	<3(-14)	<5.5(-14)	<3(-14)
1482 .....	Si I (3+4)	<1(-12)	<4(-14)	<2(-14)	7(-14)	<3(-14)	<5.5(-14)	<3(-14)
1549 .....	C IV (1)	<2(-12)	1.6(-13)	1.4(-13)	7.6(-14)	4(-14)	<5.5(-14)	<3(-14)
1561 .....	C I (3)	<2(-12)	6.5(-14)	<2(-14)	6.8(-14)	<3(-14)	<5.5(-14)	<3(-14)
1657 .....	C I (2)	<2(-12)	8.7(-14)	<3(-14)	<4(-14)	<3(-14)	<5.5(-14)	<3(-14)
1705, 1710 .....	Fe II	Satur.	<2(-13)	1.5(-13)	<4(-14)	<2(-14)	<5.5(-14)	<5(-14)
1817 .....	Si II (2)	Satur.	<2(-13)	<3.5(-14)	5.9(-14)	3.5(-14)	<5.5(-14)	<5(-14)
2796 .....	Mg II <i>k</i>	<5(-12)	1.5(-12)	1.6(-12)	...	...	...	...
2803 .....	Mg II <i>h</i>	<3(-12)	1.2(-12)	1.2(-12)	...	...	...	...
Soft X-rays .....	...	4.0(-12)	1(-12)	1.2(-12)	4.0(-12)	5.2(-13)	8.2(-13)	1.3(-12)

similarity of BD +15°640 and 70 Tau in spectral type and magnitude; however, this is not inconsistent with the errors inherent in such weak detections.

The complete absence of chromospheric or transition region line emission in the case of 71 Tau is consistent with earlier results on F stars summarized by Linsky (1981), which suggest that most F stars with  $B-V \lesssim 0.32$  do not show such line emission. As Linsky points out, however, this is not conclusive proof that early F stars lack transition regions, as the underlying bright UV

continuum makes it difficult to observe such emission. Since 71 Tau is the brightest X-ray source detected by Stern *et al.* (1981), the absence of a transition region appears unlikely.

The SWP spectra of the four G stars, BD +14°693 (G1 V), BD +16°592 (G1 V), BD +15°598 (G5 V), and BD +16°601 (G6 V), are considerably noisier due to limitations on observing time. Only the G1 dwarfs show evidence of line emission, with C IV  $\lambda 1549$  present at roughly twice the intensity in BD +14°693 as in

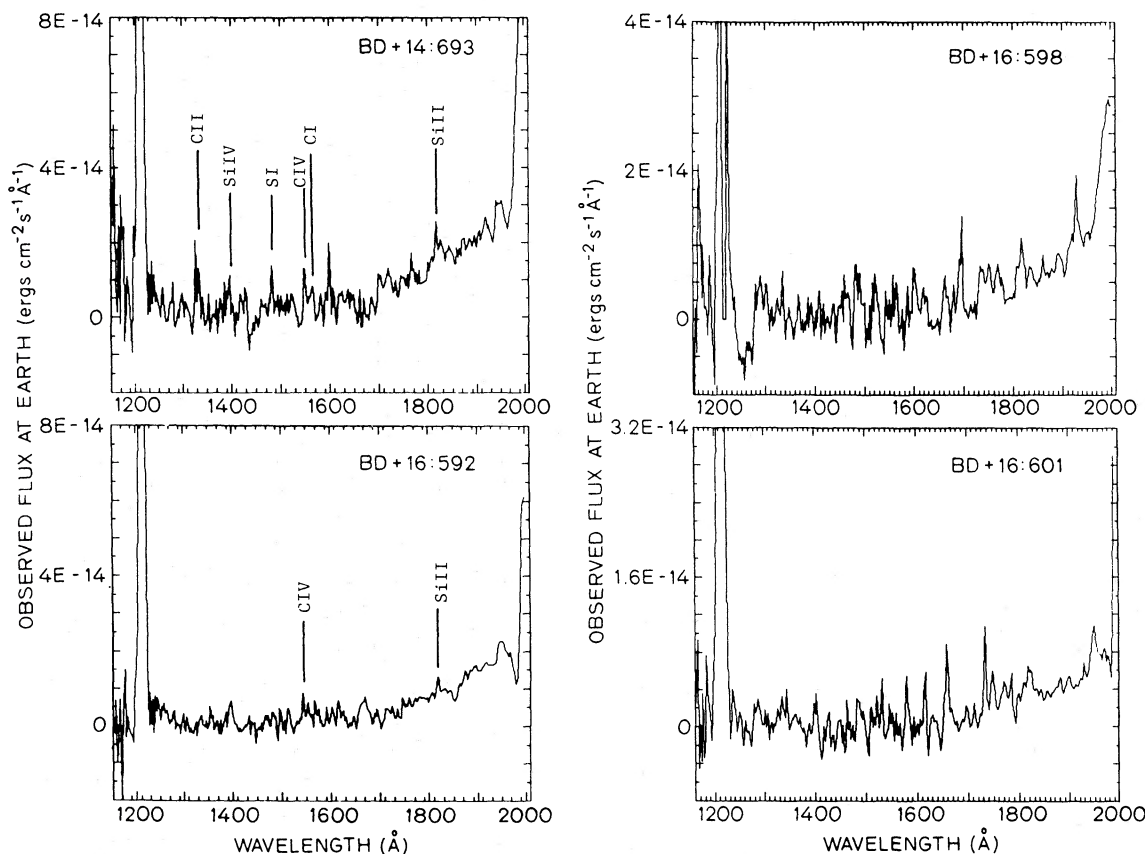


FIG. 1.—(Continued)

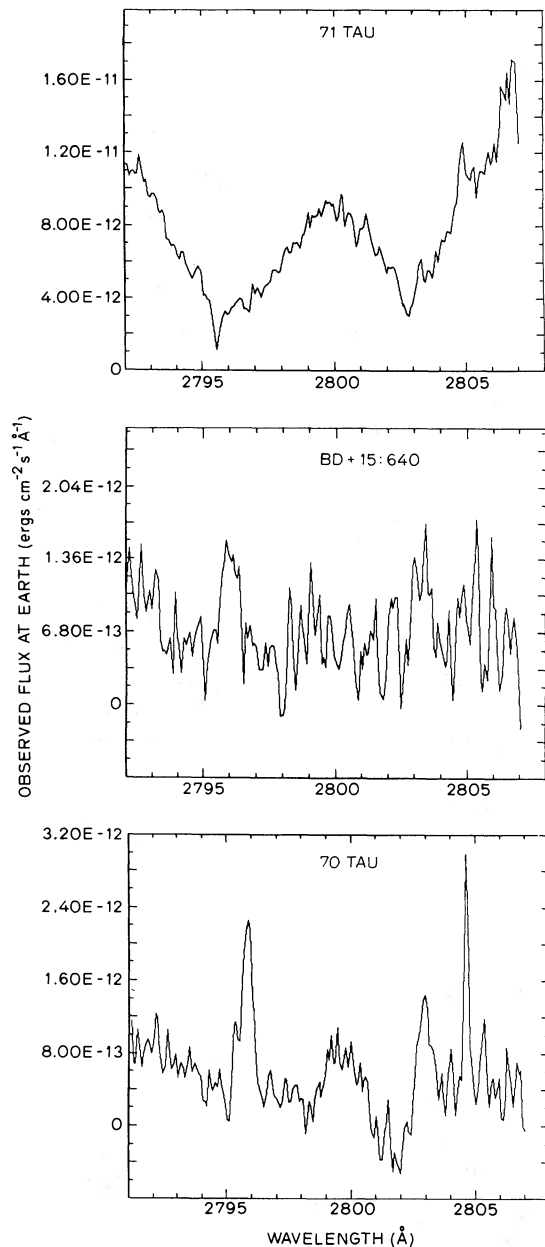


FIG. 2.—IUE long wavelength spectra of three Hyades stars: the Mg II *h* and *k* region

BD + 16°592. Although the BD + 14°693 spectrum has many instrumental noise spikes, it is possible to identify line emission due to Si IV  $\lambda 1394$  ( $T \sim 8 \times 10^4$  K), C II  $\lambda 1355$  ( $T \sim 3 \times 10^4$  K), and Si II  $\lambda\lambda 1808, 1817$  ( $T > 10^4$  K). The BD + 14°693 spectrum is particularly interesting in comparison to the solar UV spectrum plotted by Ayres, Marstad, and Linsky (1981); in the case of the Sun, the Si II blend is twice as strong as C IV, yet in the BD + 14°693 spectrum, the two sets of lines are of nearly equal strength. This suggests an enhancement of the hotter ( $T > 2 \times 10^4$  K) material relative to that of the chromosphere, as compared to the Sun. It is

important to note that the absolute flux in the C IV line seen in BD + 14°693 is about 30 times higher than that of the quiet Sun, consistent with the much higher soft X-ray flux seen in BD + 14°693. The other three stars for which C IV ( $\lambda 1540$ ) was observed all appear to be very similar in their C IV and X-ray emission (Table 4). Although this may be taken as evidence for a definite correlation between soft X-ray and C IV intensity (Ayres, Marstad, and Linsky 1981), our data set is too limited to draw any statistically significant conclusions.

We give upper limits only for the line fluxes in BD + 16°601 and BD + 16°598; these upper limits are, however, comparable to the reported fluxes for BD + 16°592. The stars BD + 16°601 and BD 16°598 are somewhat fainter and of later spectral type than BD + 16°592. The lack of detectable emission in the cooler Hyades dwarfs is probably just a selection effect due to the limited sensitivity of IUE exposures. Time variations in stellar activity may also play a role in determining the detectability of such emission.

#### b) Long-Wavelength Spectra (1900–3200 Å)

LWR spectra of 71 Tau, BD + 15°640, and 70 Tau were taken to search for the presence of Mg II *h* and *k* chromospheric emission reversal. We observed Mg II emission lines in BD + 15°640 and 70 Tau, but we failed to detect them in 71 Tau (Fig. 2). This apparent absence of Mg II emission in the 71 Tau spectrum could be due to rotational smearing of the weak emission line in the core of the strong absorption line: 71 Tau has an apparent rotational velocity of  $192 \text{ km s}^{-1}$ , leading to a  $1.9 \text{ \AA}$  broadening of an emission line at  $\sim 2800 \text{ \AA}$ . The fluxes in the observed *h* and *k* emission lines are reported in Table 3. The Mg II  $k_3$  absorption features (Fig. 2) are probably interstellar (Böhm-Vitense 1981).

Weiler and Oegerle (1979) have derived relations for the visual magnitude and the Mg II *k* emission-line luminosity as a function of the Mg II *k* emission-line width similar to the Wilson-Bappu relation. We applied their relations to the two stars for which we had positive detection of Mg II emission. We find that BD + 15°640 has about the line width and Mg II *k* luminosity expected for its spectral type; 70 Tau has a greater width and higher luminosity than expected but within the uncertainties in the observations.

Following the discussion of Linsky and Ayres (1978), we may estimate chromospheric radiative losses through the Mg II resonance line core. In the Sun, the Mg II lines contribute approximately 30% of the total radiative loss, and this ratio should not vary much, at least for solar type objects. Therefore, we may derive an upper limit for the radiative losses in 71 Tau of  $10^7 \text{ ergs cm}^{-2} \text{ s}^{-1}$ . For BD + 15°640 and 70 Tau, these radiative losses are approximately  $1.3 \times 10^7 \text{ ergs cm}^{-2} \text{ s}^{-1}$  and  $1.1 \times 10^7 \text{ ergs cm}^{-2} \text{ s}^{-1}$ , respectively. These numbers imply that BD + 15°640, 70 Tau, and 71 Tau are transforming  $1.4 \times 10^{-4}$ ,  $1.3 \times 10^{-4}$ , and less than  $6 \times 10^{-5}$  of their total luminosity (as measured by  $\sigma T_{\text{eff}}^4$ ) into mechanical energy, compared to  $5.5 \times 10^{-5}$  for the quiet Sun.

TABLE 4  
SUMMARY OF LINE SURFACE FLUXES (ergs cm<sup>-2</sup> s<sup>-1</sup>)

$\lambda(\text{\AA})$	Ion	BD + 15°640	70 Tau	BD + 14°693	BD + 16°592	Quiet Sun
1240 .....	N v (1)	<6(4)	3.3(4)	<7.6(4)	<8.9(4)	8.6(2)
1305 .....	O I (2)	<6(4)	3.2(4)	<7.6(4)	<8.9(4)	4.0(3)
1335 .....	C II (1)	1.0(5)	6.3(4)	1.5(5)	<8.9(4)	4.6(3)
1394 .....	Si IV (1)	<6(4)	<4.8(4)	1.3(5)	<8.9(4)	1.7(3)
1482 .....	Si I (3+4)	<6(4)	<2.4(4)	1.8(5)	<8.9(4)	5.3(2)
1549 .....	C IV (1)	2.4(5)	1.7(5)	1.9(5)	1.2(5)	5.8(3)
1561 .....	C I (3)	9.6(4)	<2.4(4)	1.7(5)	<8.9(4)	2.0(3)
1657 .....	C I (2)	1.3(5)	<3.6(4)	<1(5)	<8.9(4)	5.3(3)
1705, 1710 .....	Fe II	<3(5)	1.8(5)	<1(5)	<5.9(4)	...
1817 .....	Si II (2)	<3(5)	<4.2(4)	1.5(5)	1.0(5)	1.0(4)
2796 .....	Mg II <i>k</i>	2.2(6)	1.9(6)	...	...	6.0(5)
2803 .....	Mg II <i>h</i>	1.8(6)	1.4(6)	...	...	4.5(5)
Soft X-rays .....	...	1.5(6)	1.4(6)	1.0(7)	1.5(6)	...

### III. DISCUSSION

#### a) Constraints on Chromospheric and Transition Region Parameters

For optically thin lines which are collisionally excited, the power (ergs s<sup>-1</sup>) emitted in a line  $\lambda$  is given by:

$$I_{\lambda} = \int n^2 G_{\lambda}(T) d^3V, \quad (1)$$

where  $n$  is the electron density and  $G_{\lambda}$  is the excitation function of the line. Since  $G_{\lambda}$  is usually a sharply peaked function, the integral may be approximated by:

$$I_{\lambda} = 0.7 G_{\lambda}(T_{\lambda}) EM(T_{\lambda}), \quad (2)$$

where  $T_{\lambda}$  is the temperature at which  $G_{\lambda}$  peaks, and  $EM(T_{\lambda})$  is the effective emission measure at that temperature (e.g., Pottasch 1964). We have applied equation (2) to the four hottest lines in the IUE spectra for which the assumption of being optically thin is presumably valid. Table 5 gives the emission measures (EM) for the four stars for which we have positive line identifications and for the quiet-Sun. If we assume that (as is the case for the Sun), the emission originates from an isobaric, planar transition region, then the emission measure of a particular line  $\lambda$  may be approximated by:

$$EM_{\lambda} = (n_{\lambda} \cdot H_{\lambda})(P_0 \cdot \Sigma)(2kT_{\lambda})^{-1}(2\pi R^2), \quad (3)$$

where  $n_{\lambda}$  is determined by the perfect gas law  $n_{\lambda} = P_0/2kT_{\lambda}$ ;  $\Sigma$  is the fraction of the stellar surface emitting this line;  $R$  is the stellar radius; and  $H_{\lambda}$  is the scale height defined by the temperature gradient,  $T ds/dT$ , at temperature  $T_{\lambda}$ . If we further assume that the transition

region plasma is static, then the temperature scale height can be determined from the requirement that the radiative losses be sufficient to dissipate the conductive flux through the transition region (Vesceky, Antiochos, and Underwood 1979):

$$H \approx 10^{-3} n^{-1} T^{7/4} \Lambda(T)^{-1/2}, \quad (4)$$

where  $\Lambda(T)$  is the radiative loss function for optically thin emission (Cox and Tucker 1969; Raymond, Cox, and Smith 1976). In our calculations, we have approximated the radiative loss function with the following functional form:

$$\Lambda(T) = \begin{cases} 10^{-19} T^{-1/2}, & 10^5 \leq T \leq 2 \times 10^7 \text{ K} \\ 3.5 \times 10^{-27} T^{1/2}, & T \geq 2 \times 10^7 \text{ K} \end{cases} \text{ ergs cm}^3 \text{ s}^{-1}. \quad (5)$$

Combining equations (3) and (4) an expression can be derived for the product of pressure and stellar coverage at temperature  $T_{\lambda}$ :

$$(P_0 \cdot \Sigma)_{\lambda} = 2.76 \times 10^{-13} (2\pi R^2)^{-1} T_{\lambda}^{-3/4} \Lambda(T_{\lambda})^{1/2} EM_{\lambda}. \quad (6)$$

We expect equation (6) to be valid only for lines formed above the chromosphere. In the chromosphere, the dominant radiative losses are due to optically thick emission; therefore, equation (4) does not hold for  $T \lesssim 3 \times 10^4$  K. In addition, it is not likely that a static isobaric model is valid for the chromosphere. It is certainly not valid for the solar chromosphere. As a test of the model, we computed  $(P_0 \Sigma)$  using equation (6) for the observed C IV and N V lines from 70 Tau. The

TABLE 5  
EMISSION MEASURES (cm<sup>-3</sup>)

Star	EM <sub>CII</sub>	EM <sub>SiIV</sub>	EM <sub>CIV</sub>	EM <sub>NV</sub>	EM <sub>X</sub>
BD + 15°640 .....	1.24(51)	<2.49(50)	6.55(49)	<1.27(50)	6.5(50)
70 Tau .....	6.79(50)	<1.74(50)	4.06(49)	6.08(49)	7.4(50)
BD + 14°693 .....	1.42(51)	4.12(50)	3.98(49)	<1.23(50)	1.4(52)
BD + 16°592 .....	<8.43(50)	<2.83(50)	2.51(49)	<1.44(50)	1.0(51)
Quiet Sun .....	3.95(49)	4.89(48)	1.10(48)	1.28(48)	4.0(48)

results agree to better than 3%, which is well within the uncertainties in our data.

As stated previously, we assume  $P_0$  to be constant over the transition region. In addition, we will assume the stellar coverage  $\Sigma$  to be the same in the transition region (where C IV is formed) and at the base of the corona; hence:

$$(P_0 \cdot \Sigma)_{C\text{ IV}} \approx (P_0 \cdot \Sigma)_{N\text{ V}} \approx (P_0 \cdot \Sigma)_{\text{cor}}. \quad (7)$$

This is valid only as a first approximation since, if the emission originates from active region loops, as in the Sun, we expect that the loop cross section varies from the transition region to the corona. However, for simplicity, we will assume a constant loop cross section. Using equation (7) the temperature at the base of the corona can be derived; viz.,

$$\begin{aligned} [G_x(T_{\text{cor}})/\Lambda^{1/2}(T_{\text{cor}})]T_{\text{cor}}^{3/4} \\ = 2.76 \times 10^{-13}(L_x/2\pi R^2) \cdot (P_0 \cdot \Sigma)^{-1}, \quad (8) \end{aligned}$$

where  $(L_x/2\pi R^2)$  is simply the X-ray surface flux,  $G_x$  is the emissivity of the plasma in the X-ray band observed, and  $(P_0 \cdot \Sigma)$  is obtained from the UV observations, equation (6). We may now derive an upper limit on  $\Sigma$  due to the fact that the size scale of the coronal emission must be less than or of the order of the gravitational scale height:

$$\Sigma \lesssim \Sigma_{\text{max}} = 3 \times 10^{26} T_{\text{cor}}^{-7/4} \Lambda(T_{\text{cor}})^{1/2} \frac{(P_0 \cdot \Sigma)}{g}, \quad (9)$$

where  $g$  is the stellar surface gravity and can be obtained from Allen (1973).

Note that there are certain limitations inherent in equations (7) and (8). First, there is the assumption that  $\Sigma$  is the same for the corona and transition region. Second, there is the implicit assumption that the X-ray and UV observations are simultaneous. Unfortunately, this is not the case with our data sets since there is approximately a 6 month interval between the *Einstein* and the *IUE* observations. Finally, the model strictly applies to only a single coronal loop so that a unique  $T_{\text{cor}}$  and a unique  $P_0$  are possible. If, as is more likely, the emission is due to a collection of active region loops with different  $T_{\text{cor}}$  and  $P_0$ , then the values determined by equations (7) and (8) will represent some "average" loop. As long as the range of variation of  $T_{\text{cor}}$  and  $P_0$  is not too large, these average values determined by our

model will be physically significant. However, if, for example, the X-ray emission is due to a single very hot, dense loop whereas the UV emission is dominated by cool, low pressure loops, then our results will not be valid.

For the case of the Sun, equations (8) and (9) do yield reasonable values. Assuming a moderately active Sun with an X-ray luminosity of  $L_x = 10^{27.5}$  ergs  $\text{s}^{-1}$  and a coronal temperature of about  $T_{\text{cor}} = 3 \times 10^6$  K in the active regions, then equation (8) implies that  $P_0 \Sigma = 5.2 \times 10^{-2}$  dyn  $\text{cm}^{-2}$ . Using equation (9) the maximum value of the solar surface covered by active regions is  $\Sigma_{\text{max}} \approx 2\%$ , implying a minimum pressure in the transition region of  $P_{0\text{ min}} = 2.5$  dyn  $\text{cm}^{-2}$  and, therefore, an active region density at the base of the corona of  $n_{\text{cor}} = 3 \times 10^9$   $\text{cm}^{-3}$ , which agrees with observations.

We have performed the analysis described above on the four stars for which we have definite line identifications. Table 6 lists the values of the coronal parameters derived for these stars and, for comparison, a moderately active Sun with  $L_x = 3 \times 10^{27}$  ergs  $\text{s}^{-1}$ . The errors on these results are probably quite large, at least a factor of 2, due to the many uncertainties in the data and the model. However, they do provide a critical test of the hypothesis that the emission from these stars is due to a solarlike corona and transition region. The two F stars (BD +15°640 and 70 Tau) tend to have similar characteristics: cooler coronae, larger "coverage," and, hence, smaller densities than the two G Hyades dwarfs. On the other hand, the two G stars (BD +14°693 and BD +16°592) are very dissimilar: while BD +16°592 seems to be similar to the active Sun, BD +14°693 has a very hot corona ( $>10^7$  K) and a very small coverage ( $\sim 0.2\%$ ) leading to high densities, especially in the transition region. Such a small coverage would be appropriate for a star in a flaring state. However, the X-ray observations did not indicate any time variability which could be associated with a flare, although the location of this star close to the ribs of the IPC makes the interpretation difficult.

Although BD +14°693 has low values for the ultraviolet fluxes compared to its high X-ray flux, it may still be compatible with a static loop model if temporal variations are considered. Several months elapsed between the X-ray and ultraviolet observations, so that cyclic variation similar to the Sun's may have occurred. Also if, indeed, the fraction of stellar surface covered

TABLE 6  
MODEL PARAMETERS

Star	$P_0 \cdot \Sigma$ (dyn $\text{cm}^{-2}$ )	$T_{\text{cor}}$ (K)	$\Sigma_{\text{max}}$	$P_{0\text{ min}}$ (dyn $\text{cm}^{-2}$ )	$n_{0\text{ min}}$ at $T = 10^5$ K, $\text{cm}^{-3}$	$n_{\text{cor, min}}$ at $T = T_{\text{cor}}$ , $\text{cm}^{-3}$	$H_{0\text{ max}}$ (cm)
BD +15°640 .....	1.3	9.7(5)	1	1.3	4.7(10)	4.8(9)	3.8(9)
70 Tau .....	0.9	1.9(6)	1	0.9	3.3(10)	1.7(9)	1.1(11)
BD +14°693 .....	1.0	4.6(7)	2.3(-3)	4.35(2)	1.6(13)	3.4(10)	2.8(11)
BD +16°592 .....	0.65	4.3(6)	1.3(-1)	5.0	1.8(11)	4.2(9)	8.6(10)
Quiet Sun .....	$\approx 1(1-2)$	1.6(6)	5.0(-2)	0.2	7.2(9)	4.5(8)	1.3(10)
Moderately active Sun .....	5(2)	3.0(6)	2.0(-2)	2.5	9.0(10)	3.0(9)	9.9(9)

by active regions is so small, then we have to take into account the "rotational modulation." We do not have any measurements of rotational velocity for BD +14°693; however, the average value of  $v_{\text{rot}} \approx 9 \text{ km s}^{-1}$  for Hyades solar type dwarfs (Stern *et al.* 1981; Zolcinski 1981) implies that any single active region rotates in about 5 days, a time which is much longer than any X-ray or ultraviolet observation. Therefore, the case of a single active region is not excluded, and it would be impossible to associate the X-ray flux and the ultraviolet flux unless they were determined simultaneously.

It is of interest to consider the relation between coronal emission and stellar rotation. Only three stars out of four had their rotational velocities measured (see Table 1). Neglecting the anomalous case of BD +14°693, it seems that the coronal temperatures deduced from the static conductively heated loop model are essentially independent of stellar rotation. Considering the average characteristics of the Hyades stars, it seems rather that the emission measure increases with increasing rotational velocity, although our data are not reliable enough to suggest a particular functional dependence. From Table 6 it appears that the main difference between the Sun (which is an old, slow rotator) and the Hyades stars (which are young, fast rotators) is in the area covered by active regions, i.e.,  $\Sigma_{\text{max}}$ , and not in the physical characteristics of these regions. However, it should be emphasized that we are able to obtain only an upper limit on  $\Sigma$ . If, instead, one assumes that  $\Sigma$  is the same for the Sun and the Hyades, then it is the coronal pressure that increases with increasing rotational velocity.

#### b) Differential Emission Measure

The differential emission measure used in equation (2) is defined as (e.g., Antiochos 1980):

$$EM \equiv An^2H, \quad (10)$$

where  $A$  is the area of the emitting source. Assuming, as before, a static, isobaric loop with constant area, we may obtain a relation for EM as a function of temperature only:

$$EM(T) \propto T^{3/4} \Lambda(T)^{-1/2}, \quad (11)$$

where we have used equation (4). In most cases of interest, we will have  $10^5 \leq T < 2 \times 10^7 \text{ K}$ , and we may apply the first expression in equation (4) to obtain:

$$EM(T) \propto T. \quad (12)$$

This result applies only to an atmosphere containing a single loop or identical loops; however, the observed emission measure may be due to the contributions of loops at different temperatures. If all the loops are compatible with the static model, then the observed value of the slope will be less than unity since no individual loop contributes a slope steeper than unity (Antiochos 1980). Hence, we may deduce the temperature dependence of the emission measure for  $T \geq 10^5 \text{ K}$  to be  $EM \propto T^\delta$  where  $\delta \leq 1$ .

The solar emission measure is observed to agree with this prediction. In the range  $10^5 \leq T \leq 10^6$ ,  $\delta$  is observed to be less than unity (Raymond and Doyle 1981). A minimum is observed in the emission measure at  $T \approx 10^5$ , with a subsequent increase in  $EM(T)$  for cooler temperature, i.e.,  $\delta < 0$  for  $T < 10^5$ . Small or negative values of  $\delta$  may be readily understood as the effect of a collection of loops at different temperatures. In addition, the radiative loss function turns over and becomes an increasing function of  $T$  for  $T \lesssim 10^5$ . From equation (11) we note that this also has the effect of decreasing  $\delta$  (for  $T \lesssim 10^5$ ).

We have computed for BD +15°640, 70 Tau, BD +14°693, and BD +16°592 the emission measures at those temperatures in the transition region where the ions of C II, Si IV, and N V are most abundant. The results are given in Table 5. We also list the X-ray emission measures obtained from the *Einstein* observations. For comparison, the values of the emission measures of the quiet Sun, with  $L_x = 3 \times 10^{26} \text{ ergs s}^{-1}$  are given in Table 5, as well.

In order to compare the slopes of the emission measures, we normalized them by the emission measure at  $T = 10^5 \text{ K}$ , namely,  $EM_{\text{CIV}}$ . The choice of C IV as a normalization factor is purely practical: it is the only emission line for which we have positive identifications in the four Hyades stars. The results are plotted in Figure 3. It is to be noted that these curves are not model independent at the higher temperatures. The calculation of the coronal emission measure involves the knowledge of  $T_{\text{cor}}$  deduced in § IIIa using the static loop model. Hence, the slope of the differential emission measure between  $\sim 10^5 \text{ K}$  and  $T_{\text{cor}}$  equals unity, since this result is implicitly assumed in the static loop model. We expect the actual slopes to be somewhat less than unity (as in the Sun) due to the contribution of cool

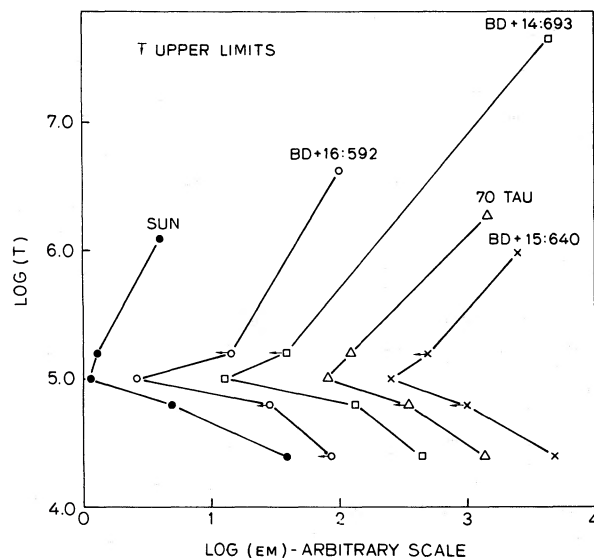


FIG. 3.—Differential emission measure for four Hyades stars and the quiet Sun in units of  $EM_{\text{CIV}}$  (emission measure at  $T = 10^5 \text{ K}$ ). Upper limits are indicated by triangles.

loops. Hence, our estimate for  $T_{\text{cor}}$  is probably only a lower limit on the true coronal temperature. Figure 3 shows also the differential emission measure for the quiet Sun, which is model independent throughout the temperature range, since  $T_{\text{cor}}$  is well determined observationally.

The first striking feature that can be seen in Figure 3 is that  $\text{EM}_{\text{CIV}}$  is minimum in all stars. This is a true minimum in the case of the Sun; however, the curves may be misleading in the case of the Hyades stars. We have only four points to construct the differential emission curves; in addition, some of these points are only upper limits (identified by arrows in Fig. 3). In the extreme case of BD +16°592, we have upper limits for all points except C IV and the X-rays. Therefore, the minimum may lie anywhere below  $T \approx 10^5$  K.

Of more interest are the results for the region below  $10^5$  K since these are model independent. As is evident from Figure 3, the differential emission measure curves in the temperature range  $3 \times 10^4 \text{ K} < T < 10^5 \text{ K}$  are very similar for the Sun and the Hyades stars (within the observational errors) so that  $\text{EM}(T) \propto T^{-2}$ . We can even extend this similarity up to  $T = 2 \times 10^5$  K for 70 Tau and the quiet Sun. Doschek *et al.* (1978) have obtained the same result for  $\alpha$  Aur, HR 1099,  $\lambda$  And,  $\epsilon$  Eri, and for several very different regions of the solar atmosphere (quiet Sun, coronal hole, active region, and flares). It appears, therefore, that while the absolute value of the emission measure may change for different stars (by a factor of 30 or more), the shape of emission measures for  $3 \times 10^4 \text{ K} < T < 10^5 \text{ K}$  seems to be the same, at least, for different regions of the Sun, the Hyades stars observed, and the stars mentioned above. We believe that this is an important result and that more observations are clearly needed to determine whether this effect holds for other stars, as well.

The observed form of  $\text{EM}(T)$  for  $T < 10^5$  (i.e.,  $\delta \approx -2$ ) does not seem to be compatible with the static loop model. Pallavicini *et al.* (1981) have performed a detailed comparison of solar observations with the standard static models and have found that they could not reproduce the observed rise in  $\text{EM}(T)$  at low temperatures. Several explanations are possible. One is that the coronal heating mechanism (whatever that may be) becomes greatly enhanced at low temperature. However, as pointed out by Craig, McClymont, and Underwood (1978), the differential emission measure predicted by the static model is essentially independent of the coronal heating function, unless one assumes a highly artificial form for this heating. Hence, we consider this possibility to be unlikely. Another explanation is that it is due to the effect of a collection of static loops with a particular distribution of loop parameters, i.e., area,  $P_0$ ,  $T_{\text{cor}}$ , etc. We also consider this to be unlikely since there is no apparent reason that the same distribution of loops should occur in vastly different regions of the Sun and on stars of different types. The most likely possibility is that the static model is not valid in this temperature range and that the form of the differential emission measure is due to the effect of mass motions. We intend to explore this possibility in a subsequent paper.

#### IV. SUMMARY OF THE ULTRAVIOLET OBSERVATIONS

The results of this paper may be summarized as follows:

1. Although the *IUE* sensitivity limit did not allow us to detect emission lines in three stars, we confirm the presence of chromospheres and transition regions in BD +15°640, 70 Tau, BD +14°693, and BD +16°592, already postulated through their X-ray emission.

2. We have observed three stars with the *IUE* long-wavelength camera and estimated the chromospheric radiative losses in BD +15°640 and 70 Tau to be roughly twice as large as in the Sun. The upper limit of the chromospheric radiative losses of 71 Tau is of the order of the Sun's value.

3. Assuming a plane-parallel transition region, one finds that the power emitted by an optically thin line is proportional to the product of the pressure and the emitting fraction of stellar surface. Assuming, in addition, a static conductively heated loop model, one may combine the ultraviolet and soft X-ray observations to derive an isothermal coronal temperature and to constrain the density, pressure, and emitting fraction of the stellar surface. With the above assumptions, we find that BD +15°640, 70 Tau, and BD +16°592 are all consistent with a static conductively heated loop model. However, BD +14°693 is not compatible with such a model unless strong temporal variations in its UV and X-ray emission and postulated.

4. We have plotted the differential emission measure as a function of temperature for the four stars mentioned above. While the absolute values of the emission measures vary by a factor of 30 between the quiet Sun and the two G Hyades dwarfs, their slopes are fairly similar: they exhibit a solar-like minimum between  $3 \times 10^4 \text{ K} \lesssim T \lesssim 2 \times 10^5 \text{ K}$ . For temperatures lower than  $T < 10^5 \text{ K}$ , the slopes are identical within the error of measurements [ $\text{EM}(T) \propto T^{-2}$ ]. For  $T > 10^5 \text{ K}$ , the possible contribution of cool loops implies that the estimated coronal temperature derived is a lower limit.

We would like to thank Dr. A. Boggess and the staff of the *IUE* Observatory for their assistance in obtaining the observations. We are in debt to A. Lane, T. R. Ayres, R. E. Stencel, P. Bornmann, and L. Caroff for their help in using the computer facilities at the Jet Propulsion Laboratory (Pasadena, Cal.), the Joint Institute for Laboratory Astrophysics (Boulder, Col.), and the NASA-Ames Research Center (Mountain View, Cal.). We would like to thank the referee for helpful comments. In addition, M-C. Zolcinski would like to express her genuine appreciation to J. L. Linsky and R. E. Stencel for their help and guidance in the ultraviolet data analysis. M-C. Zolcinski and A. B. C. Walker, Jr., were supported by NASA grants NSG 5131 and NSG 5417; S. K. Antiochos was supported by NASA grants NAGW-92 and NGL-05-020-272, and ONR contract N00014-75-C-0673; R. A. Stern was supported by NASA contract NAS 7-100.



## REFERENCES

- Allen, C. W. 1973, *Astrophysical Quantities* (3d ed.; London: Athlone Press).
- Antiochos, S. K. 1980, *Ap. J.*, **241**, 385.
- Ayres, T. R., Marstad, N. C., and Linsky, J. L. 1981, *Ap. J.*, **247**, 545.
- Barnes, T., and Evans, D. 1976, *M.N.R.A.S.*, **174**, 489.
- Böhm-Vitense, E. 1981, *Ap. J.*, **244**, 504.
- Boggess, A., et al. 1978a, *Nature*, **275**, 372.
- Boggess, A., et al. 1978b, *Nature*, **275**, 377.
- Bohlin, R. C., Holm, A. V., Savage, B. D., Sniijders, M. A. J., and Sparks, W. M. 1980, *Astr. Ap.*, **85**, 1.
- Burton, W. M., and Ridgeley, A. 1970, *Solar Phys.*, **14**, 3.
- Cox, D. P., and Tucker, W. H. 1969, *Ap. J.*, **157**, 1157.
- Craig, I. J. D., McClymont, A. N., and Underwood, J. H. 1978, *Astr. Ap.*, **70**, 1.
- Doschek, G. A., Feldman, U., Mariska, J. T., and Linsky, J. L. 1978, *Ap. J. (Letters)*, **226**, L35.
- Doschek, G. A., Feldman, U., VanHoosier, M. E., and Bartoe, J-D. F. 1976, *Ap. J. Suppl.*, **31**, 417.
- Dupree, A. K. 1981, in *Solar Phenomena in Stars and Stellar Systems*, (ed. R. M. Bonnet and A. K. Dupree (Dordrecht: Reidel), p. 407.
- Holm, A. 1979, *NASA IUE Newsletter No. 7*, 27.
- Linsky, J. L. 1981, *Solar Phenomena in Stars and Stellar Systems*, (ed. R. M. Bonnet and A. K. Dupree (Dordrecht: Reidel), p. 99.
- Linsky, J. L., and Ayres, T. R. 1978, *Ap. J.*, **220**, 619.
- Linsky, J. L., Worden, S. P., McClintock, W., and Robertson, R. M. 1979, *Ap. J. Suppl.*, **41**, 47.
- Pallavicini, R., Peres, G., Serio, S., Vaiana, G. S., Golub, L., and Rosner, R. 1981, *Ap. J.*, **247**, 692.
- Pottasch, S. R. 1964, *Space Sci. Rev.*, **3**, 816.
- Raymond, J. C., Cox, D. P., and Smith, B. W. 1976, *Ap. J.*, **204**, 290.
- Raymond, J. C., and Doyle, J. G. 1981, *Ap. J.*, submitted.
- Stern, R. A., Zolcinski, M-C., Antiochos, S. K., and Underwood, J. H. 1981, *Ap. J.*, **244**, 647.
- Vaiana, G. S., et al. 1981, *Ap. J.*, **245**, 163.
- Vesecky, J. F., Antiochos, S. K., and Underwood, J. H. 1979, *Ap. J.*, **233**, 987.
- Walter, F., and Bowyer, S. 1981, *Ap. J.*, **245**, 671.
- Weiler, E. J., and Oegerle, W. R. 1979, *Ap. J. Suppl.*, **39**, 537.
- Zolcinski, M-C. 1981, Stanford Institute for Plasma Research Report 843, Stanford, California.

S. K. ANTIOCHOS and A. B. C. WALKER, JR.: Institute for Plasma Research, Via Crespi, Stanford University, Stanford, CA 94305

R. A. STERN: MS 169-327, Jet Propulsion Laboratory, California Institute of Technology, 4800 Oak Grove Drive, Pasadena, CA 91109

M-C. S. ZOLCINSKI: University of New Hampshire, DeMeritt Hall, Physics Department, Durham, NH 03824